

# Constraints on dark axion portal: missing energy and fermion EDMs

Sergei N. Gnnienko  <sup>1,2,3</sup> N. V. Krasnikov  <sup>1,2</sup> Valery E. Lyubovitskij  <sup>4,3</sup> Sergey Kuleshov  <sup>3,5</sup>  
Alexey S. Zhevlakov  <sup>2,6</sup> I. V. Voronchikhin  <sup>1,7</sup> and D. V. Kirpichnikov  <sup>1,\*</sup>

<sup>1</sup> *Institute for Nuclear Research, 117312 Moscow, Russia*

<sup>2</sup> *Bogoliubov Laboratory of Theoretical Physics, JINR, 141980 Dubna, Russia*

<sup>3</sup> *Millennium Institute for Subatomic Physics at the High-Energy Frontier (SAPHIR) of ANID, Fernández Concha 700, Santiago, Chile*

<sup>4</sup> *Institut für Theoretische Physik, Universität Tübingen,*

*Kepler Center for Astro and Particle Physics,*

*Auf der Morgenstelle 14, D-72076 Tübingen, Germany*

<sup>5</sup> *Center for Theoretical and Experimental Particle Physics, Facultad de Ciencias Exactas, Universidad Andres Bello, Fernandez Concha 700, Santiago, Chile*

<sup>6</sup> *Matrosov Institute for System Dynamics and Control Theory SB RAS,*

*Lermontov str., 134, 664033, Irkutsk, Russia*

<sup>7</sup> *Tomsk Polytechnic University, 634050 Tomsk, Russia*

We study a model in which a new interactions between the Standard Model (SM) photon and both the dark photon ( $\gamma_D$ ) and an ALP ( $a$ ) are described by the dark axion portal operator. The implications of this dark axion portal scenario for electron fixed-target experiments are presented. In particular, we investigate the missing energy signatures associated with production of dark photons and their subsequent invisible decays into stable dark sector fermions,  $\gamma_D \rightarrow \chi\bar{\chi}$ . We discuss the discovery potential for such a scenario and derive projected sensitivity curves for the NA64e and LDMX experiments. Furthermore, novel constraints of the NA64e for  $9.37 \times 10^{11}$  electrons on target are derived by considering two production mechanisms for invisible states: (i) the bremsstrahlung-like emission of an  $a\gamma_D$  pair,  $eN \rightarrow eN\gamma^* (\rightarrow a\gamma_D)$ , and (ii) the exclusive vector meson photoproduction,  $\gamma^* N \rightarrow NV$ , followed by the invisible decays of vector mesons,  $V \rightarrow a\gamma_D$ . Additionally, the constraints on the parameter space of  $CP$ -violating, fermion-specific ALP and dark photon couplings are established. These constraints are derived from current experimental bounds on the electric dipole moments (EDMs) of SM fermions, incorporating loop-induced contributions to the EDMs of the electron, muon, and neutron.

## I. INTRODUCTION

Axion-like particles (ALP or  $a$ ) represent a well-motivated class of pseudo-scalar bosons that emerge naturally in numerous extensions of the Standard Model (SM). Originally posited as a dynamical solution to the strong  $CP$  problem, their theoretical foundation has been expanded significantly, as reviewed in [1, 2]. Beyond this primary role, ALPs provide a viable framework for addressing phenomenological puzzle, serving as viable candidates for the cosmological dark matter (DM) relic density [3–5].

The phenomenological landscape of ALPs extends to more exotic scenarios, such as those featuring lepton flavor violation. Such models, where ALPs mediate transitions between different lepton generations, have been the subject of detailed theoretical and experimental investigation [6–9]. Recent reviews and a multitude of studies, spanning beam-dump experiments, fixed-target facilities, colliders, RF cavities, and astrophysical probes, explore various signatures and constraints on these particles [10–36].

Recent work has introduced a novel interaction framework known as the dark axion portal [37, 38]. This effec-

tive operator facilitates the production of dark photons in the early Universe and, for sufficiently low-mass dark photon states, provides a viable mechanism for generating the observed cosmological dark matter relic density. The portal is characterized by vertices coupling the axion (or a generic ALP) simultaneously to the SM photon and the dark photon,  $a\gamma\gamma_D$ .

Building upon the theoretical framework proposed in Refs. [39–41], this work investigates the phenomenology of the dark axion portal in a scenario where the associated dark photon decays predominantly into dark sector (DS) states. In this model, the dark photon is identified as the gauge boson of a hidden  $U_D(1)$  symmetry, thereby acting as the primary mediator between the Standard Model and DS particles through the portal interaction.

We demonstrate that this scenario yields a rich phenomenology accessible through missing energy signatures at electron beam fixed-target experiments. Specifically, we conduct an analysis of the discovery potential for such signals at the current experiment NA64e [28–32, 42, 43] and the proposed LDMX facility [44–50].

We also develop the ideas presented in Refs. [51, 52] where the implication of light sub-GeV bosons for electric dipole moments (EDM) of fermions and  $CP$ -odd dark axion portal coupling was discussed in detail. In particular, we argue that the EDM of fermions can be induced by: (i)  $CP$ -odd Yukawa-like couplings of ALP, (ii)  $CP$ -even interaction of SM fermions and dark pho-

\* e-mail: dmbrick@gmail.com

ton and (iii)  $CP$ -even dark axion portal coupling. As a result, one can obtain bounds on the corresponding couplings.

This work is structured as follows. Sec. II details the theoretical framework and benchmark scenarios for the dark axion portal. Sec. III outlines the missing energy signatures relevant for dark matter production in fixed-target experiments. In Sec. IV we outline benchmark experiments. In Sec. V, we derive constraints on the portal's effective couplings using data from electron-beam fixed-target facilities. Sec. VI explores the generation of electric dipole moments for Standard Model fermions within dark axion portal framework incorporating additional  $CP$ -violating couplings. Finally, Section VII provides a summary and conclusions.

## II. THE DESCRIPTION OF THE BENCHMARK SCENARIOS

The coupling between dark and electromagnetic photons can be associated with ALPs through specific interaction [37, 38]. The effective Lagrangian for such non-renormalizable dark axion portal takes the form

$$\mathcal{L}_{\text{dark axion portal}} \supset \frac{g_{a\gamma\gamma_D}}{2} a F_{\mu\nu} \tilde{F}'^{\mu\nu}, \quad (1)$$

that is the interaction between ALP and both SM and dark photon, where  $F^{\mu\nu}$  and  $\tilde{F}'^{\mu\nu}$  are the stress tensors of the visible and dark photons, respectively,  $g_{a\gamma\gamma_D}$  is the coupling constant.

This work explores a benchmark extension of the dark axion portal framework by incorporating a minimal dark sector candidate. Within this model, the dark photon, emerging from a hidden  $U_D(1)$  gauge symmetry, acts as the mediator between the Standard Model sector and a dark fermionic sector. The relevant Lagrangian is given by:

$$\mathcal{L}_{\text{DS}} \supset \bar{\chi} (i\gamma^\mu D_\mu - m_\chi) \chi, \quad (2)$$

where the DS field  $\chi$  is a Dirac fermion representing a dark sector particle with mass  $m_\chi$ . Its covariant derivative is  $D_\mu = \partial_\mu + ig_D A'_\mu$ , introducing the gauge coupling  $g_D$  associated with the hidden  $U_D(1)$  charge. A key phenomenological assumption of this setup is that the dark photon decays predominantly into a pair of these dark fermions,  $A' \rightarrow \chi\bar{\chi}$ , resulting in an invisible final state thus making it interesting for searching, in particular, in fixed target experiments, such as NA64e and LDMX. The phenomenological consequences of these signatures are analyzed in Sec. II, III, IV, and V.

One can assume the existence of the the Yukawa-like couplings of the ALP with SM fermions [41, 52–55],

$$\mathcal{L}_{CP} \supset \sum_{f=e,\mu,n} g_f^a a \bar{f} f \quad (3)$$

violating the  $CP$  symmetry, thus they can induce the electric dipole moment (EDM) of SM fermions. It is

worth to estimate the bounds on the combination of couplings from the EDM of fermions in the framework of their additional model independent benchmark interactions with dark photon

$$\mathcal{L} \supset \sum_{f=e,\mu,n} e \epsilon_f A'_\mu \bar{f} \gamma^\mu f, \quad (4)$$

where protophobic cooupings  $e\epsilon_f$  of massive hidden vector can be relevant to the exotic fifth force scenarios addressing in Ref. [56].

The study of EDM fermion bounds, incorporating the Lagrangians in Eqs. (1), (3), and (4), is of particular interest in the present paper. In Sec. VI, we discuss their phenomenological implications.

## III. THE MISSING ENERGY SIGNAL

This section outlines the missing energy/momentum signatures in the  $2 \rightarrow 4$  reactions which can be searched for with the electron fixed-target experiments NA64e [28–32] and LDMX [44–49]. Specifically, the signature of interest arises from a reaction of a high-energy electron scattering on a heavy target nucleus  $N$ :

$$eN \rightarrow eNa\gamma_D, \quad (5)$$

where the scattered electron in the final state is accompanied by a significant missing energy which is carried away by the ALP,  $a$ , and dark photon,  $\gamma_D$  escaping detection.

Within the minimal dark axion portal scenario (1), one of the source of the missing energy ( $E_{\text{miss}}$ ) is the bremsstrahlung-like production of an  $a\gamma_D$  pair via an off-shell photon. The complete process,  $eN \rightarrow eN\gamma^* \rightarrow eNa\gamma_D$ , is followed by the prompt invisible decay of the dark photon,  $\gamma_D \rightarrow \bar{\chi}\chi$ , into stable dark sector fermions. A representative Feynman diagram for this mechanism is shown in Fig. 1.

While electron bremsstrahlung remains a primary mechanism for producing hidden sector particles, Ref. [48] proposes a complementary source of missing-energy signatures (see e. g. Refs. [57–60] for recent study of meson decays to DM particles at fixed-target experiments). This alternative channel implies the exclusive photoproduction of a high-energy vector meson  $V$  (such as  $\rho$ ,  $\omega$ ,  $\phi$ , or  $J/\psi$ ) on a target nucleus  $N$ , via the reaction  $\gamma^* N \rightarrow NV$ . The initial off-shell photon  $\gamma^*$  originates from standard bremsstrahlung,  $eN \rightarrow eN\gamma^*$ .

In this analysis, we focus on a specific invisible decay mode of these vector mesons. We consider the process, see Fig. 2, where a meson decays into an off-shell photon, which then converts into an ALP and a dark photon:  $V \rightarrow \gamma^* \rightarrow a\gamma_D$ . This channel provides a distinct signature of the dark axion portal, contributing to the total missing energy in the final state.

In the dark axion portal scenario, the dark photon can decay via several channels. For masses satisfying  $m_{\gamma_D} \gtrsim m_a$ , a visible two-body decay into ALP and SM photon

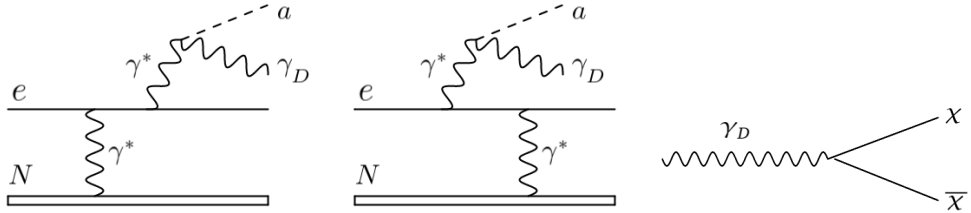


FIG. 1. Feynman diagrams illustrating the bremsstrahlung-like production of an ALP and a dark photon in electron-nucleus scattering,  $eN \rightarrow eNa\gamma_D$ . These diagrams correspond to the missing-energy signature within the minimal dark axion portal scenario, governed by the effective Lagrangian  $\mathcal{L} \supset \frac{1}{2}g_{a\gamma\gamma_D}aF_{\mu\nu}\tilde{F}^{\mu\nu}$ . In this analysis, the produced dark photon decays predominantly into invisible dark sector fermions,  $\gamma_D \rightarrow \chi\bar{\chi}$ . Diagrams involving photon emission from the nucleus line are omitted, as their contribution is suppressed by a factor of order  $(Zm_e/M_N)^2$  for electron-nucleus scattering and is therefore negligible.

becomes kinematically allowed. Its partial decay width is given by [40]:

$$\Gamma_{\gamma_D \rightarrow a\gamma} = \frac{g_{a\gamma\gamma_D}^2}{96\pi} m_{\gamma_D}^3 \left(1 - \frac{m_a^2}{m_{\gamma_D}^2}\right)^3. \quad (6)$$

Simultaneously, the Lagrangian of Eq. (2) permits an invisible decay into a pair of dark sector fermions,  $\gamma_D \rightarrow \bar{\chi}\chi$ , provided  $m_{\gamma_D} \gtrsim 2m_\chi$ . The corresponding partial width is [61]:

$$\Gamma_{\gamma_D \rightarrow \bar{\chi}\chi} = \frac{g_D^2}{12\pi} m_{\gamma_D} \left(1 + \frac{2m_\chi^2}{m_{\gamma_D}^2}\right) \left(1 - \frac{4m_\chi^2}{m_{\gamma_D}^2}\right)^{1/2}. \quad (7)$$

This work focuses on the scenario where the dark photon decays invisibly into a dark fermion pair,  $\gamma_D \rightarrow \bar{\chi}\chi$ . We assume a branching fraction  $\text{Br}_{\gamma_D \rightarrow \bar{\chi}\chi} \simeq 1$ , which is naturally satisfied for  $m_\chi \ll m_{\gamma_D}$ . This condition requires the invisible decay width to dominate over the visible channel,  $\Gamma_{\gamma_D \rightarrow \bar{\chi}\chi} \gg \Gamma_{\gamma_D \rightarrow a\gamma}$ . Consequently, a hierarchy between the couplings is implied,  $g_D \gg g_{a\gamma\gamma_D} m_{\gamma_D}$ . Under this hierarchy, any produced dark photon decays predominantly into the dark sector.

Furthermore, to ensure the invisibility of the final state within the fixed-target detector, we require the ALP mass to be significantly smaller than the dark photon mass,  $m_a \ll m_{\gamma_D}$ . This kinematically suppresses the potentially visible decay  $a \rightarrow \gamma\gamma_D$ , guaranteeing that both the ALP and the dark sector fermions escape the experiment undetected, resulting in a clean missing-energy signature.

### A. Bremstrahlung-like production: $\gamma^* \rightarrow a\gamma_D$

The expected number of missing-energy events from the process  $eN \rightarrow eN\gamma^* \rightarrow eN(a\gamma_D)$ , where the electron scatters off a target nucleus  $N$ , can be estimated as:

$$N_{\gamma^* \rightarrow a\gamma_D} \simeq \text{EOT} \cdot \frac{\rho N_A}{A} L_T \int_{E_{\min}}^{E_{\max}} dE_{\text{miss}} \frac{d\sigma_{2 \rightarrow 4}(E_e)}{dE_{\text{miss}}}. \quad (8)$$

In this expression,  $E_e$  is the initial electron beam energy,  $\text{EOT}$  is the total number of electrons on target, and  $\rho$ ,  $A$ , and  $L_T$  denote the density, atomic mass, and effective length of the target, respectively. The symbol  $N_A$  represents Avogadro's number. The differential cross section  $d\sigma_{2 \rightarrow 4}(E_e)/dE_{\text{miss}}$  describes the  $2 \rightarrow 4$  bremsstrahlung-like process  $eN \rightarrow eN\gamma^* \rightarrow eNa\gamma_D$ , and  $E_{\text{miss}} = E_a + E_{\gamma_D}$  is the total energy carried away by the invisible ALP and dark photon system. The integration limits  $E_{\min}$  and  $E_{\max}$  are set by the specific energy acceptance and selection criteria of the experimental setup.

We compute the relevant  $2 \rightarrow 4$  cross sections using the CalcHEP software package [62]. To this end, we have extended the SM implementation in CalcHEP by introducing two new massive particles: the ALP  $a$  and the dark photon  $\gamma_D$ . Their interaction with the SM photon is incorporated via the effective Lagrangian term (1). The target nucleus is modeled as a spin-1/2 particle with mass  $M_N$ , atomic mass  $A$ , and charge  $Z$ . Its coupling to the photon is implemented through the vertex factor  $ieZF(t)\gamma_\mu$ , where  $t = -q^2 > 0$  is the squared momentum transfer to the nucleus and  $F(t)$  denotes the nuclear elastic form factor. Following [63, 64], we employ the parameterization

$$F(t) = \frac{a^2 t}{1 + a^2 t} \frac{1}{1 + t/d}, \quad (9)$$

with screening and finite-size parameters given by  $a = 111Z^{-1/3}/m_e$  and  $d = 0.164A^{-2/3} \text{ GeV}^2$ . This form factor is incorporated into the analytic expression for the squared matrix element  $|\mathcal{M}_{eN \rightarrow eNa\gamma_D}|^2$  generated by CalcHEP, and the corresponding C++ source files have been modified accordingly.

Using the experimental parameters detailed in Sec. IV, we numerically integrate the exact tree-level amplitude squared for the process  $eN \rightarrow eN\gamma^*(\rightarrow a\gamma_D)$  over the full final-state phase space. This computation is performed within the CalcHEP framework. For a given target material and a fixed electron beam energy  $E_e$ , we evaluate the total cross section  $\sigma_{\text{tot}}$  as a function of the dark photon mass  $m_{\gamma_D}$ , scanning the range  $1 \text{ MeV} \lesssim m_{\gamma_D} \lesssim 1 \text{ GeV}$  while fixing the ALP mass at  $m_a \simeq 10 \text{ keV}$ .

The multidimensional phase-space integration is carried out using the VEGAS adaptive Monte Carlo algorithm. We configure the integration with  $N_{\text{session}} = 10$  independent runs, each employing  $N_{\text{calls}} = 10^6$  sampling points. The adaptive grid optimization within VEGAS achieves a numerical precision of approximately  $\mathcal{O}(0.1)\%$  to  $\mathcal{O}(0.01)\%$  in the final cross-section results.

### B. Production via vector meson decays: $V \rightarrow a\gamma_D$

The expected number of missing-energy events from the process  $eN \rightarrow eN\gamma^* \rightarrow eN(a\gamma_D)$ , where the electron scatters off a target nucleus  $N$ , can be estimated as:

$$N_V = \text{EOT} \times f_{\text{brem}} \times P_V,$$

where EOT is the total number of electrons on target,  $f_{\text{brem}}$  denotes the fraction of incident electrons that emit a hard bremsstrahlung photon capable of producing the meson, and  $P_V$  represents the probability for such a photon to undergo an exclusive photoproduction interaction on the target. Following the treatment in Ref. [48], the photoproduction probability can be approximated as

$$P_V \simeq \frac{9}{7} \frac{\sigma_0^V X_0 f_{\text{nuc}}^V}{m_p},$$

with  $X_0$  the radiation length of the target material,  $\sigma_0^V$  the exclusive photoproduction cross section on a single nucleon, and  $f_{\text{nuc}}^V$  an  $\mathcal{O}(1)$  nuclear correction factor.

For the LDMX Phase-II design, Ref. [48] estimates  $f_{\text{brem}}^{\text{LDMX}} \simeq 0.03$ . Assuming the ultimate planned integrated luminosity of  $\text{EOT} \simeq 10^{16}$ , the resulting yields for light vector mesons are

$$N_\rho \simeq 3 \times 10^{10}, \quad N_\omega \simeq 3 \times 10^9, \quad N_\phi \simeq 5 \times 10^8. \quad (10)$$

These yields correspond to a total meson production ranging from  $\mathcal{O}(10^8)$  to  $\mathcal{O}(10^{10})$  events.

For the NA64e planned statistics of  $\text{EOT} \simeq 5 \times 10^{12}$  the typical numbers of vector mesons are estimated to be [48]

$$\begin{aligned} N_\rho &\simeq 1.2 \times 10^8, \quad N_\omega \simeq 9 \times 10^6, \\ N_\phi &\simeq 8 \times 10^6, \quad N_{J/\psi} \simeq 1.1 \times 10^5, \end{aligned} \quad (11)$$

these values imply the typical fraction of hard bremsstrahlung electrons at the level of  $f_{\text{brem}}^{\text{NA64e}} \simeq 0.5$ . Remarkably, at LDMX energies,  $J/\psi$  production is kinematically forbidden. However, its coherent  $\gamma^* N \rightarrow N J/\psi$  production is kinematically allowed at the NA64e facility.

As a result, the typical signal yield associated with vector meson invisible decay into pair of ALP-dark photon particles reads

$$N_{V \rightarrow a\gamma_D} \simeq N_V \times \text{Br}_{V \rightarrow a\gamma_D}, \quad (12)$$

where  $N_V$  is the total number of the specific vector meson,  $\text{Br}_{V \rightarrow a\gamma_D}$  is the invisible branching fraction of vector meson associated with dark ALP portal scenario. Specifically, it is given by

$$\text{Br}_{V \rightarrow a\gamma_D} = \Gamma_{V \rightarrow a\gamma_D} / \Gamma_{\text{tot}}^V \quad (13)$$

where  $\Gamma_{\text{tot}}^V$  and  $\Gamma_{V \rightarrow a\gamma_D}$  are the total and invisible decay width of the vector meson, respectively. In order to calculate  $\Gamma_{V \rightarrow a\gamma_D}$ , we employ the vector meson dominance (VMD) framework [65]. The relevant mixing between ordinary SM photon,  $A_\mu$ , and vector meson,  $V_\mu$ , reads

$$\mathcal{L}_{\text{VMD}} \supset - \sum_V \frac{e m_V^2}{g_V} A_\mu V^\mu, \quad (14)$$

where  $m_V$  is a vector meson mass,  $e$  is the elementary electric charge, and  $g_V$  is a dimensionless coupling constant that can be extracted from the data on strong decays [66]. In Tab. I we collect all vector meson terms relevant for our analysis.

The amplitude for an on-shell vector meson  $V$  to decay to  $a\gamma_D$  via virtual photon  $\gamma^*$  reads

$$\mathcal{M}_{V \rightarrow a\gamma_D} = \epsilon^\mu(q) \frac{e m_V^2}{g_V} \frac{g_{a\gamma\gamma_D}}{q^2} \epsilon_{a\gamma\gamma_D} \epsilon^{\nu\lambda\rho\sigma} k_\lambda q_\rho \epsilon_\sigma^*(k), \quad (15)$$

where  $q^\rho$  and  $k^\lambda$  are the momenta of the vector meson and dark photon, respectively. Squaring and summing over final dark photon polarizations  $\epsilon_\sigma^*(k)$  and averaging over initial meson polarizations  $\epsilon_\mu(q)$  yields the decay rate in the rest frame of the meson:

$$\Gamma_{V \rightarrow a\gamma_D} = \frac{e^2 g_{a\gamma\gamma_D}^2}{96\pi} \frac{m_V^3}{g_V^2} \left( 1 - \frac{m_{\gamma_D}^2}{m_V^2} \right)^3. \quad (16)$$

To evaluate the decay width (16), we employ the FeynCalc package [67] within the Wolfram Mathematica environment [68]. This calculation assumes the mass hierarchy  $m_{\gamma_D} \gg m_a$ , allowing us to safely neglect the ALP mass, consistent with the assumptions outlined earlier.

The resulted number of missing energy events reads

$$N_{\text{sign.}} \simeq N_{\gamma^* \rightarrow a\gamma_D} + \sum_V N_{V \rightarrow a\gamma_D}. \quad (17)$$

In Fig. 3 we show the total number of  $a\gamma_D$  pairs produced at the NA64e and LDMX experiments as a function of  $m_{\gamma_D}$ .

For the LDMX, the dominant production mechanism of relatively light dark photons,  $m_{\gamma_D} \lesssim 30$  MeV, is associated with off shell photon emission,  $\gamma^* \rightarrow a\gamma_D$ , while for the heavier dark photons,  $m_{\gamma_D} \gtrsim 100$  MeV, the relevant rate is comparable with vector meson one  $V \rightarrow a\gamma_D$ , i. e. the vector mesons provide a sizable contribution to the missing energy signal. Accounting for the  $V$  meson contribution, would result in sensitivity enchantment of the LDMX to the dark ALP portal coupling,  $g_{a\gamma\gamma_D}$ , in the sub-GeV mass range,  $m_{\gamma_D} \lesssim 1$  GeV.

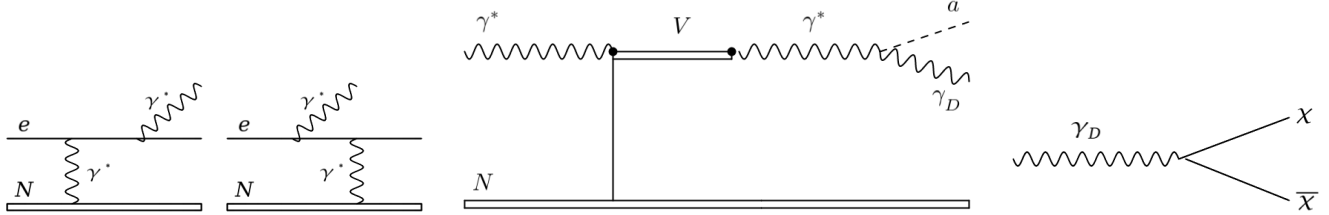


FIG. 2. Feynman diagrams for the radiative invisible vector meson decay. A hard photon  $\gamma^*$  is produced in the target,  $eN \rightarrow eN\gamma^*$ , and converts to a vector meson  $V$  in the exclusive photoproduction process  $\gamma^*N \rightarrow NV$  in the calorimeter. Then vector meson decays invisibly to the  $a\gamma_D$  pair via mixing with the ordinary off-shell photon,  $\gamma^*$ . The produced dark photon dominantly decays into invisible DS particles,  $\gamma_D \rightarrow \chi\bar{\chi}$ .

TABLE I. Parameters of vector mesons (mass  $m_V$ , coupling constant  $g_V$ , total decay width  $\Gamma_{\text{tot}}^V$ ) relevant for our analysis.

$V$	$m_V$ (MeV)	$g_V$	$\Gamma_{\text{tot}}^V$ (MeV)
$\rho$	775	4.96	147
$\omega$	782	17.3	8.6
$\phi$	1019	13.4	4.2
$J/\psi$	3097	11.8	0.093
$\Upsilon$	9460	40.3	0.054

The NA64e signal associated with coherent photoproduction of the  $J/\psi$  meson yields a rate comparable to that of  $\gamma^* \rightarrow a\gamma_D$  for sufficiently light hidden vectors, i. e. , for masses  $m_{\gamma_D} \lesssim 10$  MeV. The total number of missing energy signatures depends weakly on dark photon mass  $m_{\gamma_D}$ . This implies a sufficiently mild slope of the graph for the sub-GeV dark photons. The production of  $\rho$ ,  $\omega$  and  $\phi$  vector mesons at NA64e is subdominant for the entire mass range of interest  $1$  MeV  $\lesssim m_{\gamma_D} \lesssim 1$  GeV.

For both experiments, the yields of  $\phi$  mesons are lower than the yields of  $\omega$  mesons. Nevertheless, as shown in Fig. 3, the invisible decays of  $\phi$  mesons can provide better sensitivity due to the larger branching ratio compared to that of the  $\omega$  meson.

#### IV. BENCHMARK EXPERIMENTS

The missing energy analysis for the process  $eN \rightarrow eNa\gamma_D$  applied to both NA64e and LDMX builds upon the established frameworks developed for the related dark photon search  $eN \rightarrow eN\gamma_D$ , as detailed in Refs. [43] and [50], respectively. The experimental signatures for these two channels are nearly identical: both experiments search for events with a single scattered electron in the final state and a large missing energy, typically exceeding  $\gtrsim 50\%$  of the initial beam energy. This stringent requirement on the missing energy fraction, enabled by a fully hermetic detector design, provides a powerful tool

for suppressing standard model backgrounds.

We now outline the benchmark input parameters used for each experimental setup.

##### A. The NA64e experiment

The NA64e employs the optimized electron beam from the H4 beam line at the SPS at CERN. The maximum intensity of the beam is  $\simeq 10^7$  electrons per spill of 4.8 s, the number of good spills is estimated to be 4000 per day.

The reaction for dark photons and ALPs production,  $eN \rightarrow eNa\gamma_D$ , involves the scattering of a high-energy electron beam ( $E_e = 100$  GeV) off heavy nuclei of a lead-scintillator electromagnetic calorimeter (ECAL) serving as an active target, followed by the prompt invisible decay  $\gamma_D \rightarrow \bar{\chi}\chi$ . A significant fraction of the primary beam energy,  $E_{\text{miss}}$ , is carried away by the  $a\gamma_D$  system (and subsequently by the dark sector fermions), leaving no detectable signal in the hermetic NA64e detector. The remaining energy,  $E_e^{\text{rec}} \equiv E_e - E_{\text{miss}}$ , is deposited in the ECAL by the scattered electron. Consequently, the production of hidden particles manifests as an excess of events containing a single electromagnetic shower with energy  $E_e^{\text{rec}}$  above the expected background (see, e.g., Ref. [27]). The ECAL target of NA64e is a matrix of  $6 \times 6$  Shashlyk-type modules assembled from lead (Pb) ( $\rho = 11.34 \text{ g cm}^{-3}$ ,  $A = 207 \text{ g mole}^{-1}$ ,  $Z = 82$ ) and scintillator (Sc) plates. Note that production of hidden particles in the scintillator is subleading due to its larger radiation length,  $X_0(\text{Sc}) \gg X_0(\text{Pb})$ , thus we ignore it in the calculation.

Additionally, we assume that the electromagnetic shower in the ECAL is initiated within its typical radiation length of 0.56 cm. This defines the effective interaction length in Eq. (8) as  $L_T \simeq X_0$ , implying that the dominant production of hidden particles occurs within the initial radiation length of the active ECAL [69]. Candidate events are required to satisfy  $E_e^{\text{rec}} \lesssim 0.5E_e$ , corresponding to a lower integration limit of  $E_{\text{min}} = 50$  GeV in Eq. (8).

The dominant background sources for the NA64e missing-energy search are identified as [43]: (i) muon pair

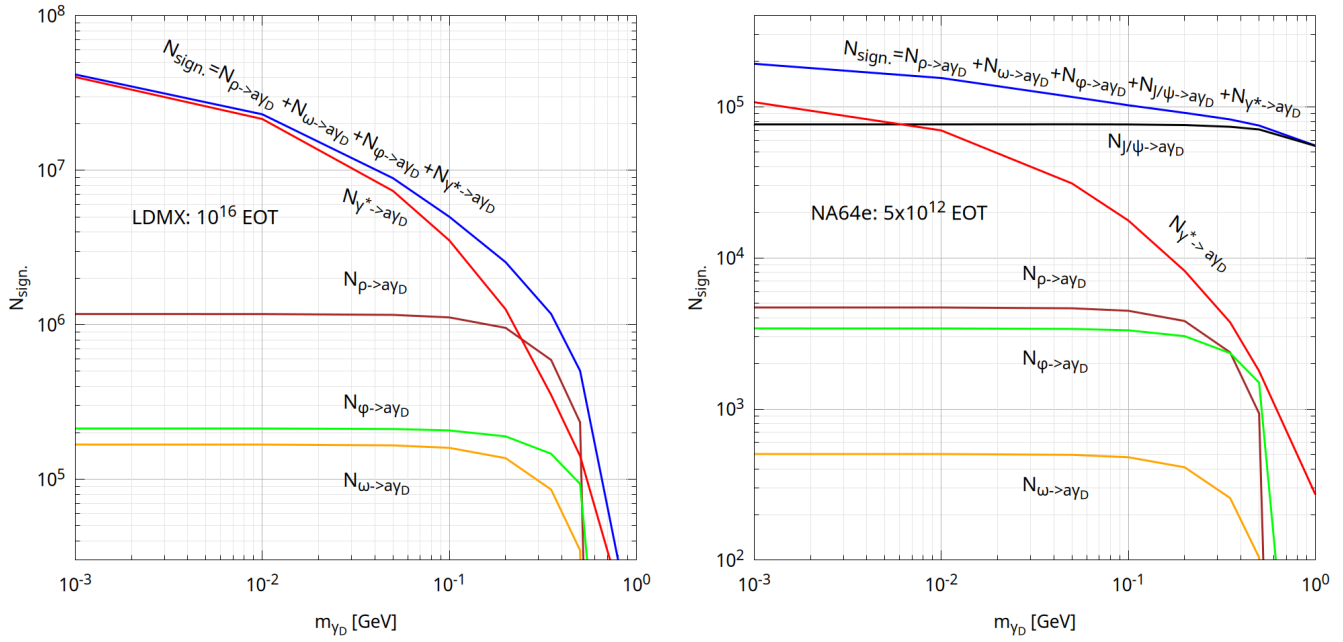


FIG. 3. The plot shows the number of  $a\gamma_D$  pairs produced versus  $\gamma_D$  mass for both LDMX ( $10^{16}$  EOT) and NA64e ( $5 \times 10^{12}$  EOT), with the coupling constant chosen to be  $g_{a\gamma\gamma_D} = 1 \text{ GeV}^{-1}$ . The hidden particles are produced in bremsstrahlung-like reactions and various meson decays. *Left panel*: the resulted number of invisible signal events for the LDMX experiment, the  $a\gamma_D$  pairs are produced through the bremsstrahlung-like channel  $\gamma^* \rightarrow a\gamma_D$  (red line), rho meson  $\rho \rightarrow a\gamma_D$  (brown line), omega meson  $\omega \rightarrow a\gamma_D$  (orange line), and phi meson decay  $\phi \rightarrow a\gamma_D$  (green line). The resulted number of  $a\gamma_D$  pairs produced at the LDMX is shown (blue line). *Right panel*: the same as in the left panel, but for the NA64e electron missing momentum facility, implying that the dominant signal mechanisms are due to the virtual photon emission  $\gamma^* \rightarrow a\gamma_D$  (red line) and  $J/\psi \rightarrow a\gamma_D$  decays (black line).

losses or decays in the target; (ii) in-flight decays along the beamline; (iii) insufficient calorimeter hermeticity; and (iv) particles passing through the calorimeter without interaction.

We adopt the background study presented in Ref. [43], which reports an estimated background of  $b \ll 1$  events for the currently accumulated exposure of  $\text{EOT} \simeq 9.37 \times 10^{11}$ . For the projected future exposure of  $\text{EOT} \lesssim 10^{13}$ , we anticipate that upgraded detector electronics and refined veto systems will improve background rejection by an  $\mathcal{O}(1)$  factor. This improvement is expected to maintain the total background at a level  $b \lesssim 1$  event, ensuring a statistically negligible background for the planned sensitivity studies with  $\simeq 10^{13}$  EOT.

## B. The LDMX experiment

The LDMX is a proposed electron fixed-target experiment at Fermilab, sharing a similar beam-based approach with NA64e. LDMX is specifically designed to reconstruct the missing momentum of the scattered electron, providing a complementary probe of the process in Eq. (5). The stringent missing-momentum requirements and extensive active veto systems employed by both experiments render them virtually background-free for the

signal topology under consideration [27, 45].

The conceptual design of LDMX comprises a thin target, a precision silicon tracker, and downstream electromagnetic and hadronic calorimeters. For detailed descriptions of the detector layout and subsystems, see Refs. [45, 49].

A significant fraction of the primary electron beam energy is lost via the emission of dark-sector particles within a thin upstream target. The resulting missing momentum of the scattered electron is reconstructed using a downstream silicon tracker system complemented by electromagnetic and hadronic calorimeters.

For the numerical analysis presented here, we consider an aluminum target with the following properties: radiation length  $X_0 = 8.9 \text{ cm}$ , density  $\rho = 2.7 \text{ g cm}^{-3}$ , atomic mass  $A = 27 \text{ g mol}^{-1}$ , and atomic number  $Z = 13$ . The effective target thickness is taken as  $L_T \simeq 0.4X_0$ . According to its design parameters, LDMX plans to accumulate an integrated luminosity of  $\text{EOT} \simeq 10^{16}$  electrons on target, with a beam energy of up to  $E_e = 8 \text{ GeV}$  during its second operational phase [48].

For the LDMX analysis, we adopt selection criteria based on prior studies searching for invisibly decaying dark photons in the sub-GeV mass range [45, 48, 49]. This approach is well justified, as the experimental signatures for the processes  $eN \rightarrow eNa\gamma_D$  and  $eN \rightarrow eN\gamma_D$

are nearly identical. The similarity arises because the differential energy spectra of the  $a\gamma_D$  system and a single dark photon share a common kinematic shape, with production dominated by the forward scattering region. Consequently, we apply the same missing-energy cut used in those references, requiring the reconstructed electron energy to satisfy  $E_e^{\text{rec}} \lesssim 0.3E_e$ . This corresponds to a lower integration limit of  $E_{\text{min}} = 0.7E_e \simeq 5.6$  GeV in Eq. (8) for an  $E_e \simeq 8$  GeV beam.

Based on current simulation studies, the residual backgrounds for LDMX originate primarily from four categories [50]: (i) unbiased electron interactions, (ii) photo-nuclear reactions, (iii) electro-nuclear interactions, and (iv) muon conversion events. To maintain sensitivity at the planned exposure of  $\text{EOT} \simeq 10^{16}$ , a targeted upgrade of the front-end electronics and trigger systems is underway [50]. The objective of these detector improvements is to achieve an effectively background-free experiment, ensuring that the projected background remains below a single event across the light dark state parameter space targeted by the benchmark search [45, 49].

## V. EXISTED AND EXPECTED SENSITIVITIES

Recent theoretical and phenomenological developments in the dark axion portal framework are summarized as follows. The regarding portal itself was formalized in Ref. [74], which proposed that the coupled system of axions and dark photons could provide a viable mechanism to account for the observed dark matter relic density [75].

Subsequently, detailed phenomenological studies have explored its experimental signatures. Ref. [39] provided a comprehensive analysis of potential signals at B-factories, fixed-target neutrino experiments, and beam-dump facilities. Further investigations have focused on specific channels: the monophoton signature arising from the decay  $\gamma_D \rightarrow a\gamma$  was examined for the experiments such as LUXE–NPOD [76], SHIP [77], FASER [78], and LHC [79] in Refs. [40, 80–82]. While a complementary analysis for reactor neutrino experiments was presented in Ref. [83]. In addition, authors of Ref. [84] proposed a scenario that connects the dark axion portal phenomenology to a potential solution for the electroweak hierarchy problem.

As emphasized previously, our analysis focuses on the scenario where the dark photon decays invisibly into dark sector fermions,  $\gamma_D \rightarrow \chi\bar{\chi}$  and  $m_{\gamma_D} > m_a$ . Consequently, the exclusion limits derived from searches for visible dark photon signatures are not directly applicable to the parameter space considered in the following subsections.

### A. Collider based constraints

An authors of Ref. [71] proposed to utilize the ATLAS as a muon fixed-target experiment. To be more specific,

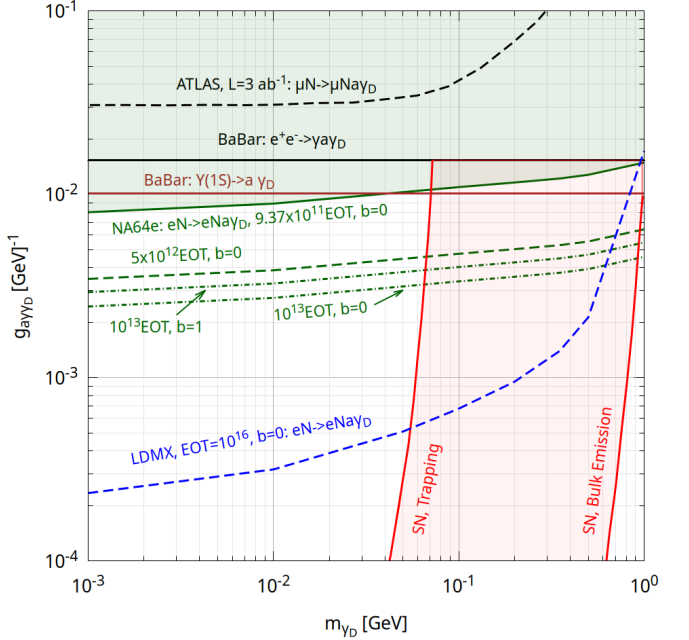


FIG. 4. The limits at 90 % CL on  $g_{a\gamma\gamma_D}$  coupling from ATLAS, BaBar, and the fixed-target experiments for the minimal dark ALP portal setup as a function of the dark photon mass  $m_{\gamma_D}$ . For the accelerator based sensitivity curves we imply that  $\text{Br}(\gamma_D \rightarrow \chi\bar{\chi}) \simeq 1$  and  $m_a = 10$  keV. Green dashed line is the projected sensitivity for NA64e experiment for  $\text{EOT} \simeq 5 \times 10^{12}$ , and blue dashed line corresponds to the projected sensitivity of LDMX facility for  $\text{EOT} \simeq 10^{16}$ . The shaded green region shows the parameter space excluded by the NA64e experiment for  $\text{EOT} \simeq 9.37 \times 10^{11}$ . For completeness, by dashed dotted green lines we show the expected reaches of NA64e for  $\text{EOT} \simeq 10^{13}$  with a finite background,  $b \simeq 1$ , and background free,  $b \simeq 0$ , case. We also show the BaBar [41] excluded bounds for the data on monophoton missing energy signature,  $e^+e^- \rightarrow \gamma a\gamma_D$ . The BaBar limits [70] from invisible decays  $\Upsilon(1S) \rightarrow a\gamma_D$  are shown by brown solid line. The projected bounds of ATLAS ( $\mathcal{L} \simeq 3 \text{ ab}^{-1}$ ) associated with muon missing momentum process,  $\mu N \rightarrow \mu N a\gamma_D$  are shown by black dashed line [71, 72]. The region of parameter space excluded by supernova (SN) is shown by shaded red area [73].

authors considered a novel analysis for the ATLAS detector, which takes advantage of the two independent muon momentum measurements by the inner detector and the muon system. They also provide the expected reach for the muon-philic sub-GeV hidden vector,  $\mathcal{L} \supset g_{\gamma_D} A'_\nu \bar{\mu} \gamma_\nu \mu$  (see e. g. left panel of Fig. 4 from Ref. [71]) in  $(m_{\gamma_D}, g_{\gamma_D})$  plane from ATLAS experiment for projected luminosity of  $\mathcal{L} \simeq 3 \text{ ab}^{-1}$ , implying muon missing momentum signature,  $\mu N \rightarrow \mu N \gamma_D$ . These limits can be relevant for our benchmark scenario, if one recasts the expected reach  $(m_{\gamma_D}, g_{\gamma_D}) \rightarrow (m_{\gamma_D}, g_{a\gamma\gamma_D})$ . Specifically, one can obtain the relevant for our analysis conservative limit on  $g_{a\gamma\gamma_D}^{\text{ATLAS}}$  from the plot shown in Fig. 4 of Ref. [71]. For the mass range of interest  $1 \text{ MeV} \lesssim m_{\gamma_D} \lesssim 1 \text{ GeV}$  the rough esti-

mate yields the following relation between couplings:

$$g_{a\gamma\gamma_D}^{\text{ATLAS}} \simeq g_{\gamma_D}^{\text{ATLAS}} \times g_{a\gamma\gamma_D}^{\text{NA64}\mu} / g_{\gamma_D}^{\text{NA64}\mu}, \quad (18)$$

where  $g_{a\gamma\gamma_D}^{\text{NA64}\mu}$  and  $g_{\gamma_D}^{\text{NA64}\mu}$  are the experimental reaches of the muon missing momentum facility NA64 $\mu$  adapted from Ref. [71] and Ref. [41], respectively for the equivalent anticipated statistics of muons accumulated on target. The conservative estimate (18) is justified by the the similar missing energy cuts and typical muon beam energies at ATLAS and NA64 $\mu$ .

In Fig. 4 we also show The BaBar excluded bounds for the data on monophoton missing energy signature,  $e^+e^- \rightarrow \gamma a\gamma_D$ , adapted from [41]. These BaBar bounds at the level of  $g_{a\gamma\gamma_D} \lesssim 1.5 \times 10^{-2} \text{ GeV}^{-1}$  rule out the projected limits of ATLAS,  $g_{a\gamma\gamma_D} \lesssim 3 \times 10^{-2} \text{ GeV}^{-1}$ , which can operate as muon missing momentum facility [71].

For the sub-GeV dark photon masses, a sufficiently strong bound,

$$g_{a\gamma\gamma_D} \lesssim 2.0 \times 10^{-2} \text{ GeV}^{-1}, \quad (19)$$

can be set from BaBar data [70] on invisible  $\Upsilon$  meson decay. Namely, the regarding branching fraction is constrained to be

$$\text{Br}_{\Upsilon \rightarrow \text{inv.}} \lesssim 3 \times 10^{-4} \quad (20)$$

at 90% CL. That limit can be associate with a relevant for our analysis bound on the invisible branching fraction of  $\Upsilon(1S) \rightarrow a\gamma_D$  vector meson. In order to extract the coupling constant bound from this limit, we employ again VMD model for  $\Upsilon(1S)$  meson, implying that typical mixing with photons is estimated to be,  $g_\Upsilon \simeq 40.3$  from its radiative decay into  $e^+e^-$  pair. Specifically, the VMD constant can be linked with leptonic decay width,  $\Gamma_{\Upsilon \rightarrow e^+e^-} \simeq 1.3 \text{ keV}$  as follows,

$$g_\Upsilon \simeq \left( \frac{4\pi\alpha^2 m_\Upsilon}{3\Gamma_{\Upsilon \rightarrow e^+e^-}} \right)^{1/2} \simeq 40.3, \quad (21)$$

where  $\alpha \simeq 1/137$  is a fine structure coupling constant,  $m_\Upsilon \simeq 9460 \text{ MeV}$  is a mass of  $\Upsilon(1S)$  meson. The resulted bound (19) is obtained by incorporating data in Tab. I, Eqs. (20) and (16). The  $\Upsilon$  invisible decay bounds (5) rule out both BaBar monophoton,  $e^+e^- \rightarrow \gamma a\gamma_D$ , limits and ATLAS muon missing energy,  $\mu N \rightarrow \mu N a\gamma_D$ , projected sensitivities.

## B. Astrophysical constraints

In this subsection we follow Ref. [73] to overview briefly other constrains on dark axion portal coupling (1) coming from the supernova bounds.

The supernova SN1987A has served as an important astrophysical laboratory for probing physics beyond the SM. The impact of novel particle emission on supernova cooling is characterized by two distinct transport

regimes, defined by the interaction strength of the new particle species. In the weak-coupling limit, particles produced in the stellar core undergo negligible re-scattering, freely escaping the proto-neutron star volume. This defines the transparent or free-streaming regime, where energy loss is proportional to the production rate. Constraints derived in this regime establish a lower bound on the particle coupling, as any stronger interaction would only enhance the emission and violate observational limits.

Conversely, if the coupling is sufficiently strong, the novel particles achieve local thermal equilibrium and become trapped within the dense medium. In this trapping regime, energy is transported diffusively and radiated from a neutrinosphere- like last scattering surface. As the coupling strength increases, this effective emission surface recedes to larger radii and lower temperatures within the stellar gradient, thereby reducing the spectral luminosity. This behavior generates an upper bound on allowable couplings, as excessively strong interactions suppress the emergent flux below levels detectable from SN1987A. The full exclusion contour, spanning from the free-streaming lower bound to the trapping upper bound, is plotted within the framework of the Raftelt criterion [85]. In Fig. 4 we show the relevant bounds by shaded red region, adapted from [73].

## C. The reach of the missing energy experiments

By using Eq. (17) to calculate the expected number of  $a\gamma_D$  production events, we derive projected exclusion limits on the portal coupling  $g_{a\gamma\gamma_D}$  within the minimal dark ALP portal framework. Assuming a background-free search ( $b \simeq 0$ ) and a null observation,  $n_{\text{obs.}} \simeq 0$ , we set a 90% confidence level (CL) exclusion criterion corresponding to a signal yield of  $N_{\text{sign.}} \gtrsim 2.3$  events. This criterion is used to determine the upper bounds on  $g_{a\gamma\gamma_D}$  presented in the following analysis.

In Fig. 4 we show the expected reach of NA64e and LDMX by green and blue solid lines, respectively. Note that projected limits on  $g_{a\gamma\gamma_D}$  from LDMX are fairly strong, i. e. for small masses of dark photon,  $m_{\gamma_D} \simeq \mathcal{O}(1) \text{ MeV}$  the expected reach is estimated to be at the level of  $g \lesssim \mathcal{O}(10^{-4}) \text{ GeV}^{-1}$ . The regarding LDMX sensitivity enchantment can be explained by the large number of the projected accumulated statistics,  $\text{EOT} \simeq 10^{16}$ , by the final phase of experimental running.

In addition, we note that the projected limits of NA64e for  $\text{EOT} \simeq 5 \times 10^{12}$  can rule the typical couplings at the level of  $g_{a\gamma\gamma_D} \lesssim (3.5-5) \times 10^{-3} \text{ GeV}^{-1}$  for sub-GeV dark photons. In Fig. 4 we show by the shaded green region the excluded limits of NA64e for the current accumulated statistics [31] of  $\text{EOT} \simeq 9.37 \times 10^{11}$ . To be more specific, the current bounds of NA64e rules out the couplings in the range  $8 \times 10^{-3} \text{ GeV}^{-1} \lesssim g_{a\gamma\gamma_D} \lesssim 1.5 \times 10^{-2} \text{ GeV}^{-1}$  for the dark photon masses of interest,  $m_{\gamma_D} \lesssim 1 \text{ GeV}$ .

To perform additional conservative projection, in

TABLE II. Upper limits on couplings of new particles from data on EDMs of electron, muon, and neutron.

Coupling combination	Electron (90 % CL)	Muon (95 % CL)	Neutron (90 % CL)
$m_{\gamma_D} = m_a \gg m_f,  g_f^a g_{a\gamma\gamma_D} e\epsilon_f  \times [\log(\Lambda^2/m_{\gamma_D}^2) + 1/2]$ :			
	$\lesssim 5.0 \times 10^{-15} \text{ GeV}^{-1}$ , $\lesssim 2.3 \times 10^{-4} \text{ GeV}^{-1}$ , $\lesssim 2.2 \times 10^{-11} \text{ GeV}^{-1}$ ,		
$m_{\gamma_D} \gg m_f \gg m_a,  g_f^a g_{a\gamma\gamma_D} e\epsilon_f  \times [\log(\Lambda^2/m_{\gamma_D}^2) + 5/2]$ :			

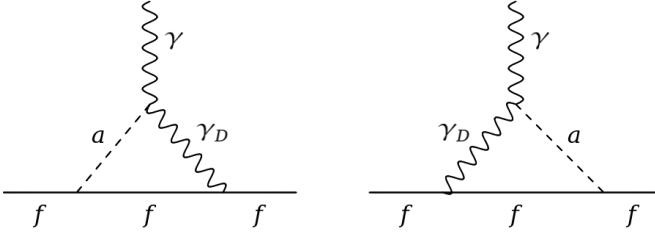


FIG. 5. Feynman diagrams which generate EDM terms due to axion coupling with both dark and SM photons (see, e. g., Eq. (22) for detail).

Fig. 4 we also show the expected reaches of NA64e implying the anticipated statistics of  $EOT \simeq 10^{13}$  for both background free,  $b = 0$ , and non-negligible number of regarding events,  $b \simeq 1$  (see, e. g., Ref. [86] and references therein for detail). To summarize principal findings of this section, we note that accounting for vector mesons would result in a sensitivity enhancement by a factor of  $\mathcal{O}(1)$  for the LDMX facility in the large mass region,  $m_{\gamma_D} \lesssim 1 \text{ GeV}$ . In contrast, for the NA64e experiment, vector meson decays enhance its sensitivity to dark ALP portal by several orders of magnitude for the sub-GeV mass range. However, a sufficiently large portion of the parameter space within,  $500 \text{ MeV} \lesssim m_{\gamma_D} \lesssim 1 \text{ GeV}$  is constrained from the SN1987A.

## VI. BOUNDS FROM FERMION EDMs

In this section, we derive the constraints on the combinations of  $P$ -even and  $P$ -odd couplings of new particles using data on electric dipole moments (EDMs) of leptons and neutron. The contributions of new particles to EDMs are described by the Bar-Zee diagrams in Fig. 5. This contribution is generated by an additional interaction Lagrangian containing three terms: (i)  $P$ -parity violating coupling of ALP with SM fermions,  $g_f^a$ , (ii)  $P$ -parity conserving coupling of ALP with SM photon and dark photon,  $g_{a\gamma\gamma_D}$ , and (iii)  $P$ -parity conserving coupling of dark photon with SM fermions,  $e\epsilon_f$ ,

$$\mathcal{L} \supset g_f^a a\bar{f}f + \frac{g_{a\gamma\gamma_D}}{2} aF_{\mu\nu}\tilde{F}'^{\mu\nu} + e\epsilon_f \bar{f}\gamma^\mu A'_\mu f. \quad (22)$$

To be more specific, the EDM of spin- $\frac{1}{2}$  fermion  $f$  (neutron or leptons) is defined as  $d_f = D_E(0, \Lambda)$ , where

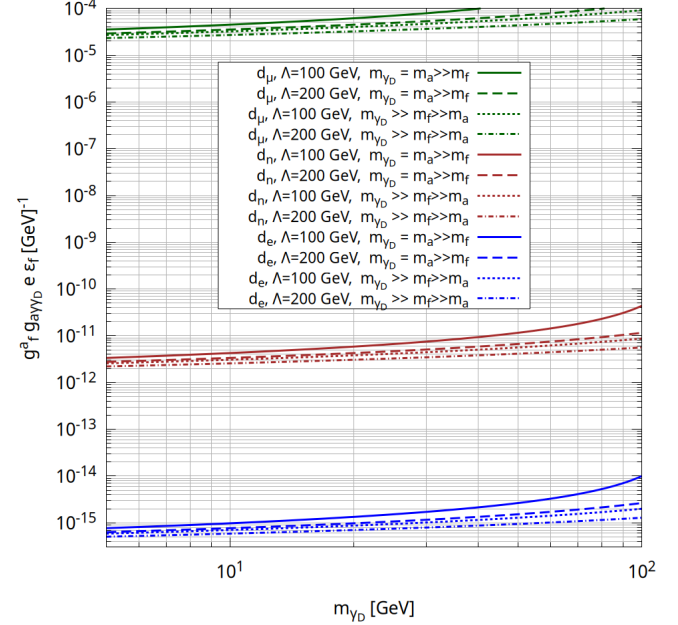


FIG. 6. Boundaries for the product of CP-odd and CP-even couplings from EDM neutron and electron/muon as the function of the dark photon mass.

$D_E(q^2, \Lambda)$  is the relativistic electric dipole form factor extracted from full electromagnetic vertex function of corresponding fermion [87–91]:

$$\begin{aligned} M_{\text{inv}} &= \bar{u}_f(p_2) \Gamma^\mu(p_1, p_2) u_f(p_1), \\ \Gamma^\mu &= -\sigma^{\mu\nu} q_\nu \gamma^5 D_E(q^2, \Lambda) + \dots, \end{aligned} \quad (23)$$

where  $q = p_1 - p_2$  is a momentum of photon. The contribution of dark axion portal depicted in Fig. 5 is divergent. With the cut-off regularization, the result in (23) is expressed in terms of the ultra-violet (UV) scale,  $\Lambda$ .

In particular, the relevant contributions of the specific diagrams in Fig. 5 read [41]

$$d_f = -\frac{G}{4\pi^2} \left[ -\frac{1}{2} + \frac{I(m_{\gamma_D}^2, m_f^2) - I(m_a^2, m_f^2)}{m_{\gamma_D}^2 - m_a^2} \right], \quad (24)$$

where  $G = g_f^a g_{a\gamma\gamma_D} e\epsilon_f$  is a product of the coupling constants, and auxiliary loop function  $I(m^2, m_f^2)$  is defined

as

$$I(m^2, m_f^2) = \int_0^1 dx \left[ m^2(1-x) + m_f^2 x^2 \right] \times \log \frac{m^2(1-x) + m_f^2 x^2}{\Lambda^2}. \quad (25)$$

Since the interaction in (1) is non-renormalizable, we treat  $\Lambda$  as scale up to which our consideration is valid. Using the upper limits/results for the electron, muon, and neutron EDMs:

$$\begin{aligned} |d_e| &< 4.1 \times 10^{-30} e \text{ cm}, & \text{at } 90\% \text{ CL, Ref. [92]}, \\ |d_\mu| &< 1.9 \times 10^{-19} e \text{ cm}, & \text{at } 95\% \text{ CL, Ref. [93]}, \\ |d_n| &< 1.8 \times 10^{-26} e \text{ cm}, & \text{at } 90\% \text{ CL, Ref. [94]}, \end{aligned}$$

we get the upper limits for combinations of couplings of new particles, which are displayed in Tab. II. We set for concreteness two benchmark cut-off scales  $\Lambda \simeq 100 \text{ GeV}$  and  $\Lambda \simeq 200 \text{ GeV}$  and plot relevant limits in Fig. 6 for the following approaches: (i) heavy dark photon with mass hierarchy,  $m_{\gamma_D} \gg m_a \gg m_f$ , (ii) equivalent mass of dark photon and ALP,  $m_{\gamma_D} = m_a \gg m_f$ .

It turns out that the electron EDM, which is currently constrained by the JILA collaboration [92] is very sensitive to probe non-minimal CP-odd dark ALP portal scenario (22) at the level of  $|g_e^a g_{a\gamma\gamma_D} e\epsilon_e| \lesssim \mathcal{O}(10^{-15}) \text{ GeV}^{-1}$ . The upper bounds on the coupling combination for the muon - and neutron- specific scenarios are estimated to be at the level of  $|g_\mu^a g_{a\gamma\gamma_D} e\epsilon_\mu| \lesssim \mathcal{O}(10^{-5}) \text{ GeV}^{-1}$  and  $|g_n^a g_{a\gamma\gamma_D} e\epsilon_n| \lesssim \mathcal{O}(10^{-12}) \text{ GeV}^{-1}$ , respectively. The bounds on the combinations of couplings depend logarithmically on dark photon mass

## VII. CONCLUSION

We have studied the missing energy signatures for the projected and existed electron fixed target experiments,

such as LDMX and NA64e. In particular, we calculated the rate of  $a\gamma_D$  pair production processes  $eN \rightarrow eNa\gamma_D$  followed by the invisible dark photon decay into DS particles  $\gamma_D \rightarrow \chi\bar{\chi}$  for the specific fixed target facility.

We derive new exclusion limits based on the NA64e data set with  $9.37 \times 10^{11}$  EOT by considering two distinct production mechanisms leading to invisible final states: (i) the bremsstrahlung-like emission of an ALP-dark photon pair,  $eN \rightarrow eN\gamma^* (\rightarrow a\gamma_D)$ , and (ii) exclusive vector meson photoproduction,  $\gamma^* N \rightarrow NV$ , followed by the invisible decay  $V \rightarrow a\gamma_D$ .

We find that vector mesons enhance sensitivity differently across experiments. For LDMX in the  $m_{\gamma_D} \lesssim 1 \text{ GeV}$  region, the enhancement factor is  $\mathcal{O}(1)$ . For NA64, vector meson decays boost sensitivity to the dark ALP portal by several orders of magnitude.

In a separate analysis, we establish constraints on the parameter space of  $CP$ -violating, fermion-specific ALP couplings. These bounds are obtained by correlating the contributions of such couplings to the electric dipole moments of the SM fermions. Specifically, we utilize current experimental limits on the EDM of SM fermions and include the associated, loop-induced contributions to the EDMs of the electron, muon, and neutron.

## ACKNOWLEDGMENTS

We would like to thank I. Galon, S. Demidov, R. Dusaev, A. Pukhov, and Y. Soreq, for very helpful discussions and correspondences. The work of V. E. L. and S. K. on deriving EDM bounds was funded by FONDECYT (Chile) under Grant No. 1240066 and by ANID–Millennium Program–ICN2019\_044 (Chile). The work of D. V. K on deriving sensitivities for both NA64e and ATLAS experiments was supported by the the Russian Science Foundation grant No. 25-12-00309.

---

[1] R. D. Peccei and Helen R. Quinn, “Constraints Imposed by CP Conservation in the Presence of Instantons,” *Phys. Rev. D* **16**, 1791–1797 (1977).

[2] Luca Di Luzio, Maurizio Giannotti, Enrico Nardi, and Luca Visinelli, “The landscape of QCD axion models,” *Phys. Rept.* **870**, 1–117 (2020), [arXiv:2003.01100 \[hep-ph\]](https://arxiv.org/abs/2003.01100).

[3] C. Boehm and Pierre Fayet, “Scalar dark matter candidates,” *Nucl. Phys. B* **683**, 219–263 (2004), [arXiv:hep-ph/0305261](https://arxiv.org/abs/hep-ph/0305261).

[4] Matthew J. Dolan, Felix Kahlhoefer, Christopher McCabe, and Kai Schmidt-Hoberg, “A taste of dark matter: Flavour constraints on pseudoscalar mediators,” *JHEP* **03**, 171 (2015), [Erratum: JHEP 07, 103 (2015)], [arXiv:1412.5174 \[hep-ph\]](https://arxiv.org/abs/1412.5174).

[5] Yonit Hochberg, Eric Kuflik, Robert McGehee, Hitoshi Murayama, and Katelin Schutz, “Strongly interacting massive particles through the axion portal,” *Phys. Rev. D* **98**, 115031 (2018), [arXiv:1806.10139 \[hep-ph\]](https://arxiv.org/abs/1806.10139).

[6] C. Han, M. L. López-Ibáñez, A. Melis, O. Vives, and J. M. Yang, “Anomaly-free leptophilic axionlike particle and its flavor violating tests,” *Phys. Rev. D* **103**, 035028 (2021), [arXiv:2007.08834 \[hep-ph\]](https://arxiv.org/abs/2007.08834).

[7] Hooman Davoudiasl, Roman Marcarelli, and Ethan T. Neil, “Lepton-Flavor-Violating ALPs at the Electron-Ion Collider: A Golden Opportunity,” (2021), [arXiv:2112.04513 \[hep-ph\]](https://arxiv.org/abs/2112.04513).

[8] S. N. Ginenko and N. V. Krasnikov, “Leptonic scalar portal: the origin of muon  $g - 2$  anomaly and dark matter?” (2022), [arXiv:2202.04410 \[hep-ph\]](https://arxiv.org/abs/2202.04410).

[9] Martin Bauer, Matthias Neubert, Sophie Renner, Marvin Schnubel, and Andrea Thamm, “The Low-Energy Effective Theory of Axions and ALPs,” *JHEP* **04**, 063 (2021), [arXiv:2012.12272 \[hep-ph\]](#).

[10] Kiwoon Choi, Sang Hui Im, and Chang Sub Shin, “Recent Progress in the Physics of Axions and Axion-Like Particles,” *Ann. Rev. Nucl. Part. Sci.* **71**, 225–252 (2021), [arXiv:2012.05029 \[hep-ph\]](#).

[11] R. R. Dusaev, D. V. Kirpichnikov, and M. M. Kirsanov, “Photoproduction of axionlike particles in the NA64 experiment,” *Phys. Rev. D* **102**, 055018 (2020), [arXiv:2004.04469 \[hep-ph\]](#).

[12] D. Banerjee *et al.* (NA64), “Search for Axionlike and Scalar Particles with the NA64 Experiment,” *Phys. Rev. Lett.* **125**, 081801 (2020), [arXiv:2005.02710 \[hep-ex\]](#).

[13] Hiroyuki Ishida, Shinya Matsuzaki, and Yoshihiro Shigekami, “New perspective in searching for axionlike particles from flavor physics,” *Phys. Rev. D* **103**, 095022 (2021), [arXiv:2006.02725 \[hep-ph\]](#).

[14] Yasuhito Sakaki and Daiki Ueda, “Searching for new light particles at the international linear collider main beam dump,” *Phys. Rev. D* **103**, 035024 (2021), [arXiv:2009.13790 \[hep-ph\]](#).

[15] Vedran Brdar, Bhaskar Dutta, Wooyoung Jang, Doojin Kim, Ian M. Shoemaker, Zahra Tabrizi, Adrian Thompson, and Jaehoon Yu, “Axionlike Particles at Future Neutrino Experiments: Closing the Cosmological Triangle,” *Phys. Rev. Lett.* **126**, 201801 (2021), [arXiv:2011.07054 \[hep-ph\]](#).

[16] Dmitry Salnikov, Petr Satunin, D. V. Kirpichnikov, and Maxim Fitkevich, “Examining axion-like particles with superconducting radio-frequency cavity,” *JHEP* **03**, 143 (2021), [arXiv:2011.12871 \[hep-ph\]](#).

[17] Dmitry Salnikov, Petr Satunin, and D. V. Kirpichnikov, “Probing axion-like particles with RF cavities separated by a thin barrier,” *Phys. Lett. B* **873**, 140142 (2026), [arXiv:2405.04983 \[hep-ph\]](#).

[18] Yonatan Kahn, Bianca Giaccone, Andrei Lunin, Alexandr Netepenko, Roman Pilipenko, and Michael Wentzel, “Searching for axions and light-by-light scattering with superconducting RF cavities,” *Proc. SPIE Int. Soc. Opt. Eng.* **12016**, 29 (2022).

[19] Luc Darmé, Federica Giacchino, Enrico Nardi, and Mauro Raggi, “Invisible decays of axion-like particles: constraints and prospects,” *JHEP* **06**, 009 (2021), [arXiv:2012.07894 \[hep-ph\]](#).

[20] P. S. Bhupal Dev, Doojin Kim, Kuver Sinha, and Yongchao Zhang, “PASSAT at future neutrino experiments: Hybrid beam-dump-helioscope facilities to probe light axionlike particles,” *Phys. Rev. D* **104**, 035037 (2021), [arXiv:2101.08781 \[hep-ph\]](#).

[21] H. Abramowicz *et al.*, “Conceptual design report for the LUXE experiment,” *Eur. Phys. J. ST* **230**, 2445–2560 (2021), [arXiv:2102.02032 \[hep-ex\]](#).

[22] Jean-François Fortin, Huai-Ke Guo, Steven P. Harris, Doojin Kim, Kuver Sinha, and Chen Sun, “Axions: From magnetars and neutron star mergers to beam dumps and BECs,” *Int. J. Mod. Phys. D* **30**, 2130002 (2021), [arXiv:2102.12503 \[hep-ph\]](#).

[23] Kento Asai, Sho Iwamoto, Yasuhito Sakaki, and Daiki Ueda, “New physics searches at the ILC positron and electron beam dumps,” *JHEP* **09**, 183 (2021), [arXiv:2105.13768 \[hep-ph\]](#).

[24] Nikita Blinov, Elizabeth Kowalczyk, and Margaret Wynne, “Axion-like particle searches at DarkQuest,” *JHEP* **02**, 036 (2022), [arXiv:2112.09814 \[hep-ph\]](#).

[25] I. Larin *et al.* (PrimEx), “A New Measurement of the  $\pi^0$  Radiative Decay Width,” *Phys. Rev. Lett.* **106**, 162303 (2011), [arXiv:1009.1681 \[nucl-ex\]](#).

[26] S. N. Gnenko, N. V. Krasnikov, M. M. Kirsanov, and D. V. Kirpichnikov, “Missing energy signature from invisible decays of dark photons at the CERN SPS,” *Phys. Rev. D* **94**, 095025 (2016), [arXiv:1604.08432 \[hep-ph\]](#).

[27] D. Banerjee *et al.* (NA64), “Search for invisible decays of sub-GeV dark photons in missing-energy events at the CERN SPS,” *Phys. Rev. Lett.* **118**, 011802 (2017), [arXiv:1610.02988 \[hep-ex\]](#).

[28] S. N. Gnenko, D. V. Kirpichnikov, M. M. Kirsanov, and N. V. Krasnikov, “The exact tree-level calculation of the dark photon production in high-energy electron scattering at the CERN SPS,” *Phys. Lett. B* **782**, 406–411 (2018), [arXiv:1712.05706 \[hep-ph\]](#).

[29] S. N. Gnenko, D. V. Kirpichnikov, M. M. Kirsanov, and N. V. Krasnikov, “Combined search for light dark matter with electron and muon beams at NA64,” *Phys. Lett. B* **796**, 117–122 (2019), [arXiv:1903.07899 \[hep-ph\]](#).

[30] D. Banerjee *et al.*, “Dark matter search in missing energy events with NA64,” *Phys. Rev. Lett.* **123**, 121801 (2019), [arXiv:1906.00176 \[hep-ex\]](#).

[31] Yu. M. Andreev *et al.*, “Improved exclusion limit for light dark matter from e+e- annihilation in NA64,” *Phys. Rev. D* **104**, L091701 (2021), [arXiv:2108.04195 \[hep-ex\]](#).

[32] Yu. M. Andreev *et al.* (NA64), “Constraints on New Physics in Electron  $g - 2$  from a Search for Invisible Decays of a Scalar, Pseudoscalar, Vector, and Axial Vector,” *Phys. Rev. Lett.* **126**, 211802 (2021), [arXiv:2102.01885 \[hep-ex\]](#).

[33] Nikita Blinov, Gordana Krnjaic, and Douglas Tuckler, “Characterizing Dark Matter Signals with Missing Momentum Experiments,” *Phys. Rev. D* **103**, 035030 (2021), [arXiv:2010.03577 \[hep-ph\]](#).

[34] Tegan D. Beattie *et al.*, “Construction and Performance of the Barrel Electromagnetic Calorimeter for the GlueX Experiment,” *Nucl. Instrum. Meth. A* **896**, 24–42 (2018), [arXiv:1801.03088 \[physics.ins-det\]](#).

[35] Andrey L. Pankratov *et al.*, “Search for dark-matter axions beyond the quantum limit: The cosmological axion Sarov haloscope proposal,” *Phys. Rev. D* **112**, 035003 (2025), [arXiv:2506.18595 \[hep-ph\]](#).

[36] Krzysztof Jodłowski, “Dark axion portal at Z boson factories,” *JHEP* **08**, 022 (2025), [arXiv:2411.19196 \[hep-ph\]](#).

[37] Kunio Kaneta, Hye-Sung Lee, and Seokhoon Yun, “Portal Connecting Dark Photons and Axions,” *Phys. Rev. Lett.* **118**, 101802 (2017), [arXiv:1611.01466 \[hep-ph\]](#).

[38] Kunio Kaneta, Hye-Sung Lee, and Seokhoon Yun, “Dark photon relic dark matter production through the dark axion portal,” *Phys. Rev. D* **95**, 115032 (2017), [arXiv:1704.07542 \[hep-ph\]](#).

[39] Patrick deNiverville, Hye-Sung Lee, and Min-Seok Seo, “Implications of the dark axion portal for the muon  $g-2$ , B factories, fixed target neutrino experiments, and beam dumps,” *Phys. Rev. D* **98**, 115011 (2018), [arXiv:1806.00757 \[hep-ph\]](#).

[40] Patrick deNiverville and Hye-Sung Lee, “Implications of the dark axion portal for SHiP and FASER and the advantages of monophoton signals,” *Phys. Rev. D* **100**, 055017 (2019), [arXiv:1904.13061 \[hep-ph\]](#).

[41] Alexey S. Zhevlov, Dmitry V. Kirpichnikov, and

Valery E. Lyubovitskij, “Implication of the dark axion portal for the EDM of fermions and dark matter probing with NA64e, NA64 $\mu$ , LDMX, M3, and BaBar,” *Phys. Rev. D* **106**, 035018 (2022), arXiv:2204.09978 [hep-ph].

[42] Yu. M. Andreev *et al.* (NA64), “Searching for Light Dark Matter and Dark Sectors with the NA64 experiment at the CERN SPS,” (2025), arXiv:2505.14291 [hep-ex].

[43] Yu. M. Andreev *et al.* (NA64), “Search for Light Dark Matter with NA64 at CERN,” *Phys. Rev. Lett.* **131**, 161801 (2023), arXiv:2307.02404 [hep-ex].

[44] Jeremiah Mans (LDMX), “The LDMX Experiment,” *EPJ Web Conf.* **142**, 01020 (2017).

[45] Asher Berlin, Nikita Blinov, Gordan Krnjaic, Philip Schuster, and Natalia Toro, “Dark Matter, Millicharges, Axion and Scalar Particles, Gauge Bosons, and Other New Physics with LDMX,” *Phys. Rev. D* **99**, 075001 (2019), arXiv:1807.01730 [hep-ph].

[46] Torsten Åkesson *et al.* (LDMX), “Light Dark Matter eXperiment (LDMX),” (2018), arXiv:1808.05219 [hep-ex].

[47] Artur M. Ankowski, Alexander Friedland, Shirley Weishi Li, Omar Moreno, Philip Schuster, Natalia Toro, and Nhan Tran, “Lepton-Nucleus Cross Section Measurements for DUNE with the LDMX Detector,” *Phys. Rev. D* **101**, 053004 (2020), arXiv:1912.06140 [hep-ph].

[48] Philip Schuster, Natalia Toro, and Kevin Zhou, “Probing invisible vector meson decays with the NA64 and LDMX experiments,” *Phys. Rev. D* **105**, 035036 (2022), arXiv:2112.02104 [hep-ph].

[49] Torsten Åkesson *et al.*, “Current Status and Future Prospects for the Light Dark Matter eXperiment,” in *2022 Snowmass Summer Study* (2022) arXiv:2203.08192 [hep-ex].

[50] Torsten Åkesson *et al.* (LDMX), “LDMX - The Light Dark Matter eXperiment,” (2025), arXiv:2508.11833 [hep-ex].

[51] D. V. Kirpichnikov, Valery E. Lyubovitskij, and Alexey S. Zhevlakov, “Implication of hidden sub-GeV bosons for the  $(g-2)_\mu$ ,  ${}^8\text{Be}$ - ${}^4\text{He}$  anomaly, proton charge radius, EDM of fermions, and dark axion portal,” *Phys. Rev. D* **102**, 095024 (2020), arXiv:2002.07496 [hep-ph].

[52] D. V. Kirpichnikov, Valery E. Lyubovitskij, and Alexey S. Zhevlakov, “Constraints on CP-odd ALP couplings from EDM limits of fermions,” *Particles* **3**, 719–728 (2020), arXiv:2004.13656 [hep-ph].

[53] Y. V. Stadnik, V. A. Dzuba, and V. V. Flambaum, “Improved Limits on Axionlike-Particle-Mediated P, T-Violating Interactions between Electrons and Nucleons from Electric Dipole Moments of Atoms and Molecules,” *Phys. Rev. Lett.* **120**, 013202 (2018), arXiv:1708.00486 [physics.atom-ph].

[54] V. A. Dzuba, V. V. Flambaum, I. B. Samsonov, and Y. V. Stadnik, “New constraints on axion-mediated P, T-violating interaction from electric dipole moments of diamagnetic atoms,” *Phys. Rev. D* **98**, 035048 (2018), arXiv:1805.01234 [physics.atom-ph].

[55] Victor Flambaum, Simon Lambert, and Maxim Pospelov, “Scalar-tensor theories with pseudoscalar couplings,” *Phys. Rev. D* **80**, 105021 (2009), arXiv:0902.3217 [hep-ph].

[56] Jonathan L. Feng, Bartosz Fornal, Iftah Galon, Susan Gardner, Jordan Smolinsky, Tim M. P. Tait, and Philip Tanedo, “Protophobic Fifth-Force Interpretation of the Observed Anomaly in  ${}^8\text{Be}$  Nuclear Transitions,” *Phys. Rev. Lett.* **117**, 071803 (2016), arXiv:1604.07411 [hep-ph].

[57] Avik Banerjee, Riccardo Catena, and Taylor R. Gray, “Magnetic Dipole Portal Vector Dark Matter at Fixed-Targets,” (2025), arXiv:2511.23259 [hep-ph].

[58] Sergei N. Gninenko, Dmitry V. Kirpichnikov, Sergey Kuleshov, Valery E. Lyubovitskij, and Alexey S. Zhevlakov, “Test of the vector portal with dark fermions in the charge-exchange reactions in the NA64 experiment at CERN SPS,” *Phys. Rev. D* **109**, 075021 (2024), arXiv:2312.01703 [hep-ph].

[59] Alexey S. Zhevlakov, Dmitry V. Kirpichnikov, Sergei N. Gninenko, Sergey Kuleshov, and Valery E. Lyubovitskij, “Probing invisible vector meson decay mode with the hadronic beam in the NA64 experiment at SPS CERN,” *Phys. Rev. D* **108**, 115005 (2023), arXiv:2309.09347 [hep-ph].

[60] A. S. Zhevlakov, V. E. Lyubovitskij, D. V. Kirpichnikov, S. Kuleshov, and S. N. Gninenko, “Studying Dark Photon Models in Decays of Neutral Mesons,” *Phys. Part. Nucl.* **56**, 500–505 (2025).

[61] M. Bondi, A. Celentano, R. R. Dusaev, D. V. Kirpichnikov, M. M. Kirsanov, N. V. Krasnikov, L. Marsicano, and D. Shchukin, “Fully Geant4 compatible package for the simulation of Dark Matter in fixed target experiments,” *Comput. Phys. Commun.* **269**, 108129 (2021), arXiv:2101.12192 [hep-ph].

[62] Alexander Belyaev, Neil D. Christensen, and Alexander Pukhov, “CalcHEP 3.4 for collider physics within and beyond the Standard Model,” *Comput. Phys. Commun.* **184**, 1729–1769 (2013), arXiv:1207.6082 [hep-ph].

[63] James D. Bjorken, Rouven Essig, Philip Schuster, and Natalia Toro, “New Fixed-Target Experiments to Search for Dark Gauge Forces,” *Phys. Rev. D* **80**, 075018 (2009), arXiv:0906.0580 [hep-ph].

[64] Yung-Su Tsai, “AXION BREMSSTRAHLUNG BY AN ELECTRON BEAM,” *Phys. Rev. D* **34**, 1326 (1986).

[65] Heath Bland O’Connell, B. C. Pearce, Anthony William Thomas, and Anthony Gordon Williams, “ $\rho - \omega$  mixing, vector meson dominance and the pion form-factor,” *Prog. Part. Nucl. Phys.* **39**, 201–252 (1997), arXiv:hep-ph/9501251.

[66] S. Navas *et al.* (Particle Data Group), “Review of particle physics,” *Phys. Rev. D* **110**, 030001 (2024).

[67] Vladyslav Shtabovenko, Rolf Mertig, and Frederik Orelana, “New Developments in FeynCalc 9.0,” *Comput. Phys. Commun.* **207**, 432–444 (2016), arXiv:1601.01167 [hep-ph].

[68] Wolfram Research, Inc., “Mathematica, Version 13.0.0,” Champaign, IL, 2021.

[69] Xiaoyong Chu, Josef Pradler, and Lukas Semmelrock, “Light dark states with electromagnetic form factors,” *Phys. Rev. D* **99**, 015040 (2019), arXiv:1811.04095 [hep-ph].

[70] Bernard Aubert *et al.* (BaBar), “A Search for Invisible Decays of the Upsilon(1S),” *Phys. Rev. Lett.* **103**, 251801 (2009), arXiv:0908.2840 [hep-ex].

[71] Iftah Galon, Enrique Kajamovitz, David Shih, Yotam Soreq, and Shlomit Tarem, “Searching for muonic forces with the ATLAS detector,” *Phys. Rev. D* **101**, 011701 (2020), arXiv:1906.09272 [hep-ph].

[72] Georges Aad *et al.* (ATLAS), “Muon reconstruction performance of the ATLAS detector in proton–proton collision data at  $\sqrt{s} = 13$  TeV,” *Eur. Phys. J. C* **76**, 292 (2016), arXiv:1603.05598 [hep-ex].

[73] Anson Hook, Gustavo Marques-Tavares, and Clayton Ristow, “Supernova constraints on an axion-photon-dark photon interaction,” *JHEP* **06**, 167 (2021), [arXiv:2105.06476 \[hep-ph\]](#).

[74] Juan Cortabitarte Gutiérrez, Bradley J. Kavanagh, Núria Castelló-Mor, Francisco J. Casas, Jose M. Diego, Enrique Martínez-González, and Rocío Vilar Cortabitarte, “Cosmology and direct detection of the Dark Axion Portal,” (2021), [arXiv:2112.11387 \[hep-ph\]](#).

[75] Paola Arias, Bastian Diaz Saez, and Joerg Jaeckel, “Freezing-in the pure dark axion portal,” *JCAP* **06**, 060 (2025), [arXiv:2501.17234 \[hep-ph\]](#).

[76] Zhaoyu Bai *et al.*, “New physics searches with an optical dump at LUXE,” *Phys. Rev. D* **106**, 115034 (2022), [arXiv:2107.13554 \[hep-ph\]](#).

[77] Sergey Alekhin *et al.*, “A facility to Search for Hidden Particles at the CERN SPS: the SHiP physics case,” *Rept. Prog. Phys.* **79**, 124201 (2016), [arXiv:1504.04855 \[hep-ph\]](#).

[78] Jonathan L. Feng *et al.*, “The Forward Physics Facility at the High-Luminosity LHC,” (2022), [arXiv:2203.05090 \[hep-ex\]](#).

[79] Georges Aad *et al.* (ATLAS), “Search for displaced photons produced in exotic decays of the Higgs boson using 13 TeV pp collisions with the ATLAS detector,” *Phys. Rev. D* **108**, 032016 (2023), [arXiv:2209.01029 \[hep-ex\]](#).

[80] Noam Ness and Barry Cimring, “Exploring the Dark Axion Portal in the LUXE-NPOD Experiment,” (2025), [arXiv:2512.11975 \[hep-ph\]](#).

[81] Krzysztof Jodłowski, “Probing some photon portals to new physics at intensity frontier experiments,” *Phys. Rev. D* **108**, 115017 (2023), [arXiv:2305.05710 \[hep-ph\]](#).

[82] Paola Arias, Bastián Díaz Sáez, Lucía Duarte, Joel Jones-Pérez, Walter Rodriguez, and Danilo Zegarra Herrera, “Probing displaced (dark)photons from low re-heating freeze-in at the LHC,” *JHEP* **01**, 135 (2026), [arXiv:2507.15930 \[hep-ph\]](#).

[83] Patrick Deniverville, Hye-Sung Lee, and Young-Min Lee, “New searches at reactor experiments based on the dark axion portal,” *Phys. Rev. D* **103**, 075006 (2021), [arXiv:2011.03276 \[hep-ph\]](#).

[84] Valerie Domcke, Kai Schmitz, and Tevong You, “Cosmological Relaxation through the Dark Axion Portal,” (2021), [arXiv:2108.11295 \[hep-ph\]](#).

[85] G. G. Raffelt, *Stars as laboratories for fundamental physics: The astrophysics of neutrinos, axions, and other weakly interacting particles* (1996).

[86] Sergei N. Gninenko, N. V. Krasnikov, Sergey Kuleshov, Valery E. Lyubovitskij, P. Crivelli, D. V. Kirpichnikov, L. Molina Bueno, Alexey S. Zhevlakov, H. Sieber, and I. V. Voronchikhin, “Probing millicharged particles with NA64 $\mu$  and LDMX,” (2025), [arXiv:2505.04295 \[hep-ph\]](#).

[87] Thomas Gutsche, Astrid N. Hiller Blin, Sergey Kovalenko, Serguei Kuleshov, Valery E. Lyubovitskij, Manuel J. Vicente Vacas, and Alexey Zhevlakov, “CP-violating decays of the pseudoscalars  $\eta$  and  $\eta'$  and their connection to the electric dipole moment of the neutron,” *Phys. Rev. D* **95**, 036022 (2017), [arXiv:1612.02276 \[hep-ph\]](#).

[88] Alexey S. Zhevlakov, Thomas Gutsche, and Valery E. Lyubovitskij, “Updated limits on the CP violating  $\eta\pi\pi$  and  $\eta'\pi\pi$  couplings derived from the neutron EDM,” *Phys. Rev. D* **99**, 115004 (2019), [arXiv:1904.08154 \[hep-ph\]](#).

[89] Alexey S. Zhevlakov, Mikhail Gorchtein, Astrid N. Hiller Blin, Thomas Gutsche, and Valery E. Lyubovitskij, “Bounds on rare decays of  $\eta$  and  $\eta'$  mesons from the neutron EDM,” *Phys. Rev. D* **99**, 031703 (2019), [arXiv:1812.00171 \[hep-ph\]](#).

[90] Claudio Dib, Amand Faessler, Thomas Gutsche, Sergey Kovalenko, Jan Kuckei, Valery E. Lyubovitskij, and Kem Pumsa-ard, “The Neutron electric dipole form-factor in the perturbative chiral quark model,” *J. Phys. G* **32**, 547–564 (2006), [arXiv:hep-ph/0601144](#).

[91] Amand Faessler, Thomas Gutsche, Sergey Kovalenko, and Valery E. Lyubovitskij, “Hadronic electric dipole moments in R-parity violating supersymmetry,” *Phys. Rev. D* **73**, 114023 (2006), [arXiv:hep-ph/0604026](#).

[92] Tanya S. Roussy *et al.*, “An improved bound on the electron’s electric dipole moment,” *Science* **381**, adg4084 (2023), [arXiv:2212.11841 \[physics.atom-ph\]](#).

[93] G. W. Bennett *et al.* (Muon (g-2)), “An Improved Limit on the Muon Electric Dipole Moment,” *Phys. Rev. D* **80**, 052008 (2009), [arXiv:0811.1207 \[hep-ex\]](#).

[94] C. Abel *et al.*, “Measurement of the Permanent Electric Dipole Moment of the Neutron,” *Phys. Rev. Lett.* **124**, 081803 (2020), [arXiv:2001.11966 \[hep-ex\]](#).